# Fluorine-enhanced boron diffusion in germanium-preamorphized silicon

J. M. Jacques[a] and K. S. Jones
*Department of Materials Science and Engineering, University of Florida, Gainesville, Florida 32611*

L. S. Robertson, A. Li-Fatou, and C. M. Hazelton
*Texas Instruments Inc., Dallas, Texas 75243*

E. Napolitani
*Istituto Nazionale per la Fisica della Materia-Materials and Technologies for Information and Communication Science (INFM-MATIS) and Dipartimento di Fisica, via Marzolo 8, I-35131 Padova, Italy*

L. M. Rubin
*Axcelis Technologies, Beverly, Massachusetts 01915*

(Received 12 April 2005; accepted 26 August 2005; published online 11 October 2005)

Silicon wafers were preamorphized with 60 keV $Ge^+$ or 70 keV $Si^+$ at a dose of $1\times10^{15}$ atoms/cm$^2$. $F^+$ was then implanted into some samples at 6 keV at doses ranging from $1\times10^{14}$ to $5\times10^{15}$ atoms/cm$^2$, followed by $^{11}B^+$ implants at 500 eV, $1\times10^{15}$ atoms/cm$^2$. Secondary-ion-mass spectrometry confirmed that fluorine enhances boron motion in germanium-preamorphized materials in the absence of annealing. The magnitude of boron diffusion scales with increasing fluorine dose. Boron motion in as-implanted samples occurs when fluorine is concentrated above $1\times10^{20}$ atoms/cm$^3$. Boron atoms are mobile in as-implanted, amorphous material at concentrations up to $1\times10^{19}$ atoms/cm$^3$. Fluorine directly influences boron motion only prior to activation annealing. During the solid-phase epitaxial regrowth process, fluorine does not directly influence boron motion, it simply alters the recrystallization rate of the silicon substrate. Boron atoms can diffuse in germanium-amorphized silicon during recrystallization at elevated temperatures without the assistance of additional dopants. Mobile boron concentrations up to $1\times10^{20}$ atoms/cm$^3$ are observed during annealing of germanium-preamorphized wafers. © *2005 American Institute of Physics*. [DOI: 10.1063/1.2084336]

## INTRODUCTION

Over the years, there has been significant interest in fluorine and boron co-implantation for the formation of ultrashallow *p*-type junctions. Of the nonmetals investigated, fluorine has the unique ability of significantly inhibiting boron transient enhanced diffusion (TED), while continuously increasing boron solubility limits during high-temperature furnace annealing and rapid thermal annealing (RTA).[1–3] During low-temperature annealing, fluorine exerts a relatively negligible influence upon boron motion when a germanium preamorphization is used.[4,5]

Duffy *et al.*[4] recently reported the phenomena of enhanced boron diffusion in germanium-preamorphized silicon during solid-phase epitaxial regrowth (SPER) annealing. In contrast to the results of Duffy *et al.*, this work shows a significant impact of the presence of fluorine on as-implanted boron profiles prior to annealing. In Figs. 1 and 2 of Duffy *et al.*, the boron secondary-ion-mass spectroscopy (SIMS) profiles appear identical in shape, whether boron is implanted alone or co-implanted with fluorine into amorphous material. When utilizing a deep preamorphization implant, such as 75 keV $Ge^+$, subsequent boron concentration profiles are typically Gaussian in nature and rather abrupt. Profile footing is a term used to describe motion that is limited to the tail portion of dopant concentration profiles. Footing of the boron profiles is only observed when (i) boron channeling occurs in crystalline silicon material[6–11] or (ii) when fluorine is incorporated.[5,12] The latter distinction applies directly to the experimental data of Duffy *et al.*, but is not observed. Their samples containing boron alone (Fig. 1 of Ref. 3) should be abrupt and smooth, footing should only be seen in samples co-implanted with fluorine (Fig. 2 of Ref. 3). In both self- and germanium-preamorphized materials, our as-implanted boron concentration profiles are Gaussian and smooth. Profile footing is only seen in the presence of fluorine, as expected. The mechanism by which footing occurs is subsequently addressed.

At present, germanium is the preamorphization species of choice over silicon, because it generates fewer defects and damage beyond the resultant amorphous/crystalline (*a*/*c*) interface and requires a much lower implant dose to amorphize silicon.[13,14] Previous works have utilized silicon and germanium preamorphizations relatively interchangeably when investigating boron diffusion characteristics, focusing on boron motion during annealing. This approach ignores the possibility that boron diffusion characteristics are highly dependent on the preamorphization species. As the semiconductor industry moves toward activation processes that inhibit additional dopant motion,[15–22] the characteristics of as-implanted dopant profiles will ultimately define junction depth. In this study, we characterize the role of fluorine in regards to boron diffusion in germanium and silicon preamorphized silicon

[a]Electronic mail: jjacques@ufl.edu

 

prior to activation annealing. In addition, we quantify the function of fluorine during the solid-phase epitaxial regrowth process.

## EXPERIMENTAL CONDITIONS

Ten (100) *n*-type Czochralski silicon wafers were commercially implanted at room temperature. Wafers were preamorphized with either germanium ions at 60 keV or silicon ions at 70 keV at a uniform dose of $1\times10^{15}$ atoms/cm$^2$. Cross-sectional transmission electron microscopy (XTEM) analysis and variable angle spectroscopic ellipsometry (VASE) confirmed amorphous layer depths of approximately 930 and 1500 Å, respectively. The amorphized wafers were then implanted with 6 keV $F^+$ at doses ranging from $1\times10^{14}$ to $5\times10^{15}$ atoms/cm$^2$ and subsequent drift mode 500 eV, $1\times10^{15}$ atoms/cm$^2$ $^{11}B^+$ co-implants. Fluorine was always implanted prior to the boron to eliminate any potential implant recoil effects.[23] Sample annealing occurred at a temperature of 550 °C in a quartz tube furnace under an $N_2$ ambient.

SIMS was performed at stage temperatures of both 25 and −75 °C. Boron SIMS profiles were obtained at room temperature (25 °C) using a CAMECA IMS-6f tool with an $O_2^+$ primary beam at a nominal current ranging from 50 to 70 nA. The beam was maintained 50° from the sample normal with a net impact energy of 800 eV. The primary beam was rastered over a $200\times200$ $\mu$m$^2$ area, with ions collected from the center 15% of the area. A constant $O_2$ ambient was maintained with a sputter rate ranging from 0.08 to 0.1 nm/s. Fluorine counts were generated at 25 °C under $Cs^+$-ion bombardment at an incident angle of 60°, current of 100 nA, and net impact energy of 1 keV. Secondary ions were obtained from the center 15% of the rastered area. Boron SIMS profiles were also generated at low temperature (−75 °C) using a CAMECA IMS-4f tool equipped with a liquid-nitrogen-thermoresistance temperature-controlled stage. The specific SIMS analysis parameters employed have been detailed previously by Napolitani *et al.*[24,25]

## RESULTS

SIMS profiles for as-implanted boron and fluorine obtained under room-temperature conditions are illustrated in Fig. 1. The projected range of the 6 keV fluorine implants is approximately 160 Å,[26] corresponding to the tail region of the subsequent boron implants. In this figure we observe dramatic footing in the tail region of the boron profiles for those samples co-implanted with fluorine. The magnitude of anomalous deviation from the sample containing boron alone scales with increasing fluorine implant dose. When fluorine is co-implanted, boron atoms are mobile in as-implanted material up to a concentration of $1\times10^{19}$ atoms/cm$^3$ (Fig. 1).

Figure 2 clearly shows the magnitude of boron motion prior to annealing resulting from the presence of fluorine. The level of motion is represented as the difference in depth between a given co-implanted sample and the reference sample containing boron alone, at a particular boron concentration. For junctions defined at the boron concentration of $1\times10^{18}$ atoms/cm$^3$, the as-implanted profiles are up to 90 Å deeper when co-implanted with fluorine at doses reaching $5\times10^{15}$ atoms/cm$^2$. However, the fluorine dose for a 6 keV implant does not appreciably influence the as-implanted boron profile for concentrations equal to or above $1\times10^{19}$ atoms/cm$^3$.

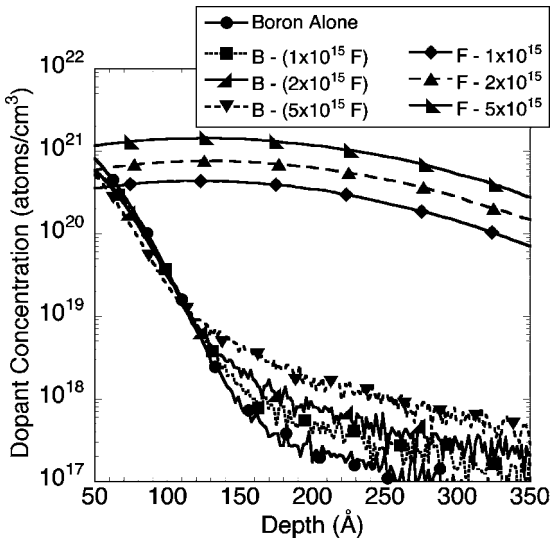


FIG. 1. Room-temperature (25 °C) dopant concentration profiles for as-implanted samples receiving 6 keV fluorine at doses ranging from $1\times10^{15}$ to $5\times10^{15}$ atoms/cm$^2$ and co-implanted with 500 eV, $1\times10^{15}$ atoms/cm$^2$ boron.

It is vital to note that the footing of the boron profiles is maintained during subsequent annealing. Figure 3 illustrates the boron diffusion characteristics resulting from a 15 min anneal at 550 °C. During the first 15 min of the SPER anneal, the boron profiles reside completely within amorphous material. The $a/c$ interface is maintained more than 300 Å below the surface in all cases, such that no appreciable interaction with the boron has occurred during annealing. In the concentration range of $1\times10^{18}$–$1\times10^{20}$ atoms/cm$^3$, boron exhibits the same diffusivity during annealing. The footings in the boron concentration profiles are distinctly maintained

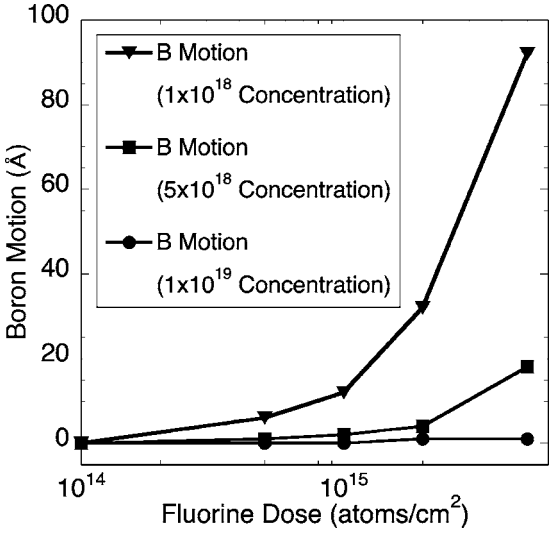


FIG. 2. Boron motion at concentrations ranging from $1\times10^{18}$ to $1\times10^{19}$ atoms/cm$^3$ in as-implanted samples with 6 keV fluorine at varied doses.

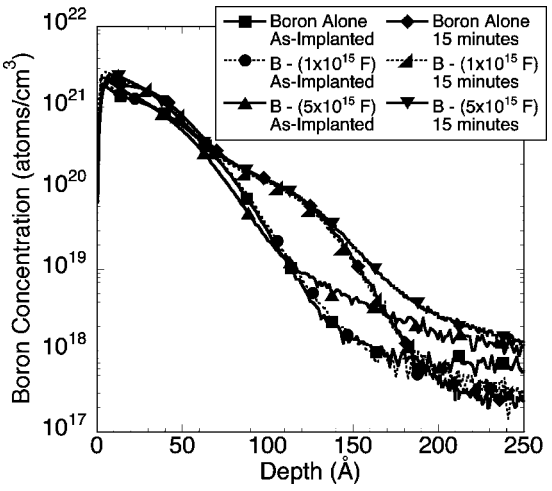


FIG. 3. Room-temperature (25 °C) boron concentration profiles for samples annealed at 550 °C for 15 min. Samples received 6 keV fluorine at doses of $1\times10^{15}$ and $5\times10^{15}$ atoms/cm$^2$, co-implanted with 500 eV, $1\times10^{15}$ atoms/cm$^2$ boron.

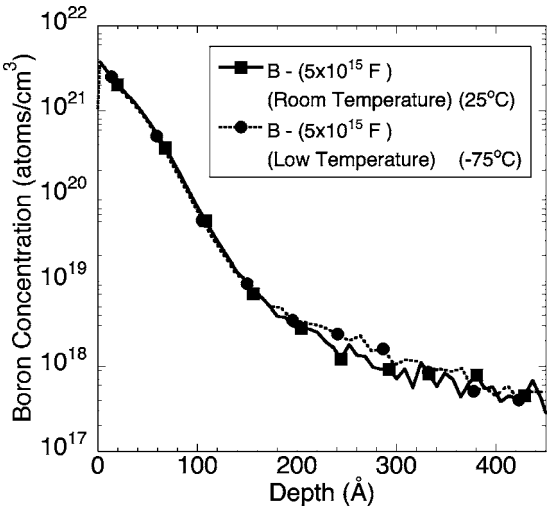


FIG. 5. Room-temperature (25 °C) and low-temperature (−75 °C) boron concentration profiles for as-implanted samples co-implanted with 6 keV, $5\times10^{15}$ atoms/cm$^2$ fluorine and 500 eV, $1\times10^{15}$ atoms/cm$^2$ boron.

during diffusion at elevated temperatures, due to the flow of boron atoms from the highly concentrated surface area into the lower concentrations below. The accompanying fluorine profiles (not shown) demonstrate minimal redistribution during annealing. The boron atoms diffuse a set magnitude irrespective of the co-implanted fluorine dose, indicating that boron can inherently diffuse in germanium-amorphized silicon during SPER. Fluorine does not directly influence boron motion under these conditions.

For longer anneal times at 550 °C, the boron profiles in these samples begin to deviate from one another (Fig. 4). This is because fluorine retards the recrystallization rate of amorphous silicon, while boron greatly enhances it.[27–30] After 30 min of annealing, the SPER process has ended for the control sample and samples co-implanted with fluorine at doses less than $1\times10^{15}$ atoms/cm$^2$. Samples co-implanted with the higher fluorine doses exhibit greater levels of boron

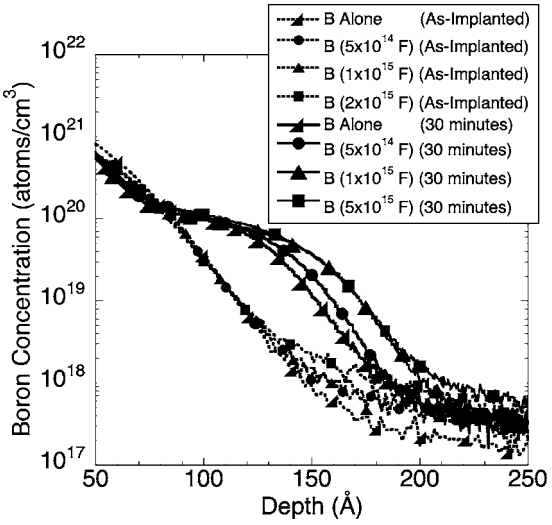


FIG. 4. Room-temperature (25 °C) boron concentration profiles for samples annealed at 550 °C for 30 min. Samples received 6 keV fluorine at doses ranging from $1\times10^{14}$ to $2\times10^{15}$ atoms/cm$^2$, co-implanted with 500 eV, $1\times10^{15}$ atoms/cm$^2$ boron.

diffusion simply due to interactions between fluorine atoms and the $a/c$ interface.[31] These interactions increase the time required to completely recrystallize the silicon substrate,[31] exposing boron to amorphous material at high temperatures for longer times. The role of fluorine co-implants during the SPER process is simply to alter the silicon regrowth rate, thereby only indirectly influencing the boron diffusion characteristics.

## DISCUSSION

Figure 1 indicates that the presence of highly concentrated fluorine enhances boron diffusion in germanium-preamorphized material during boron implantation. To address the potential for contamination resulting from the SIMS analysis itself, the analysis was repeated at the much lower stage temperature of −75 °C. During analysis, surface sputtering by the primary beam can lead to localized defect injection, thereby providing sufficient conditions for boron atoms to become mobile.[25] The presence of fluorine could possibly exacerbate these effects by enhancing boron motion at room temperature. We observed no significant variation between boron profiles obtained at the different stage temperatures, under otherwise identical analysis parameters, for both high and low fluorine dose samples. Figure 5 shows both room-temperature (25 °C) and low-temperature (−75 °C) boron concentration profiles for samples co-implanted with 6 keV, $5\times10^{15}$ atoms/cm$^2$ fluorine. These profiles are very similar and indicate a comparable level of profile footing. This data is representative of fluorine doses at 6 keV ranging up to $5\times10^{15}$ atoms/cm$^2$ and demonstrates that the fluorine-enhanced boron diffusion observed in as-implanted samples is not an artifact of SIMS analysis.

Our experiments demonstrate fluorine-enhanced boron diffusion in germanium-preamorphized silicon prior to activation annealing. When fluorine is implanted prior to boron at doses as low as $1\times10^{15}$ atoms/cm$^2$, anomalous boron motion is observed in comparison to conditions where boron is implanted alone. The enhanced motion of the boron tail

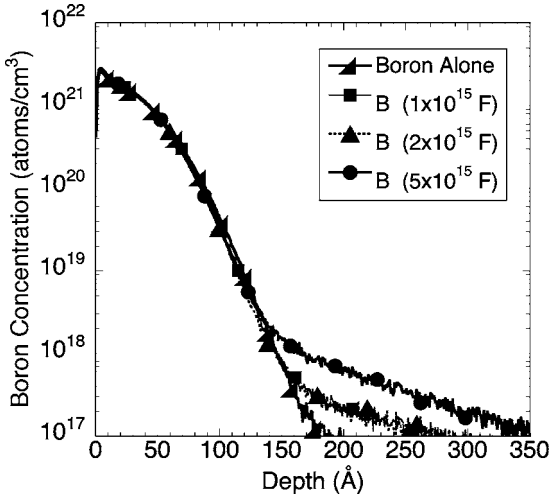


FIG. 6. Room-temperature (25 °C) dopant concentration profiles for as-implanted samples receiving 6 keV fluorine at doses ranging from $1\times10^{15}$ to $5\times10^{15}$ atoms/cm$^2$, co-implanted with 500 eV, $1\times10^{15}$ atoms/cm$^2$ boron (70 keV, $1\times10^{15}$ atoms/cm$^2$ $Si^+$ preamorphization).

region increases in magnitude as the fluorine dose increases. Fluorine has been attributed with the ability to passivate dangling and strained silicon bonds within amorphous material,[2,32] suggesting that fluorine can enhance boron motion by bonding with silicon. We observed similar boron profile footing in self-amorphized silicon. Figure 6 illustrates the as-implanted boron profiles for samples receiving a 70 keV, $1\times10^{15}$ atoms/cm$^2$ $Si^+$ preamorphization implant. The fluorine profiles (not shown) are indistinguishable from those in Fig. 1. The resulting continuous surface amorphous layer was approximately 1500 Å deep. At a boron concentration of $1\times10^{18}$ atoms/cm$^3$, the difference between the highest fluorine dose sample and the control is less than 20 Å. The magnitude of boron motion at this concentration is approximately 80% lower in self-amorphized material, as compared to germanium amorphized material, indicative of less pronounced profile footing. At higher boron concentrations, all profiles exhibit no measurable deviation from the control sample. In addition, the magnitude of the as-implanted motion does not sequentially increase with the fluorine dose, as samples co-implanted with $1\times10^{15}$ and $2\times10^{15}$ atoms/cm$^2$ fluorine at 6 keV are identical. Boron in germanium-preamorphized samples exhibits roughly five times more motion and includes an overall shift of the entire boron concentration profiles (Figs. 1 and 2). This suggests that fluorine-silicon interactions do not account for all of the anomalous boron diffusion that occurs in germanium-amorphized materials.

The combination of a germanium preamorphization and a fluorine co-implant appears to facilitate boron motion, implying that a complex chemical relationship exists between germanium, fluorine, and silicon. Prior to activation annealing, both fluorine and germanium are believed to effectively enhance boron mobility by binding with dangling and strained silicon bonds.[2,32–34] Electron-spin resonance (ESR) shows that pure evaporated amorphous silicon is homogeneously infused with dangling bonds on the order of $1\times10^{19}$ sites/cm$^3$.[35] Exposure to hydrogen plasma at elevated temperatures can completely eliminate the dangling silicon bond signal as detected by ESR.[36] Infrared (IR)-absorption spectral band analysis confirmed that hydrogenated films possess simple Si–H vibrations, demonstrating the dangling-bond density was decreased via hydrogen passivation.[36] Thus, the level of hydrogen incorporation in amorphous silicon can serve as a strong indication of the dangling-bond defect density for the material. Amorphous silicon can be permeated with hydrogen concentrations up to $1\times10^{20}$ atoms/cm$^3$.[37] The discrepancy between these two values is attributed to the belief that hydrogen can also be captured during high-temperature plasma exposure by weak bonds present throughout the amorphous structure.[37] Similar studies have not been conducted in amorphous silicon formed via ion implantation. However, if it is reasonable to extend the aforementioned defect densities to amorphous silicon generated by ion implantation, dangling silicon bond defects will exist on a level of approximately $1\times10^{19}$ sites/cm$^3$.

We observed boron atoms to be mobile in as-implanted, germanium-preamorphized silicon up to very high concentrations. At implant doses reaching $5\times10^{15}$ atoms/cm$^2$, fluorine alone only partially eliminates the dangling-bond population, primarily impacting the boron tail region. As shown in Fig. 6, the incorporation of fluorine alone facilitates limited boron diffusion, which is confined to very low boron concentrations at depths greater than 140 Å. However, these dangling bonds can be expunged when both germanium and fluorine atoms collectively bind with them, enabling boron to move at concentrations exceeding $1\times10^{19}$ atoms/cm$^3$ and depths as shallow as the substrate surface (Fig. 1). In these samples, the surface concentration of the germanium preamorphization implant exceeds $1\times10^{18}$ atoms/cm$^3$. At sample depths ranging from 100 to 500 Å, where boron profile footing is observed, germanium remains concentrated above $1\times10^{19}$ atoms/cm$^3$. The removal of defect sites and potential trapping sites in the near surface regions of implanted samples is believed to facilitate the observed boron motion.[33,34,38] Fundamental investigations of ion implantation have shown maximum lattice damage and defect generation to occur close to the substrate surface, where the distribution is generally Gaussian in nature.[38] In Fig. 7 the simulated damage profile for a 6 keV, $5\times10^{15}$ atoms/cm$^2$ fluorine implant into amorphous silicon is shown.[26] For reference, experimental boron and fluorine dopant concentration profiles are also included for samples implanted with boron alone and co-implanted with $5\times10^{15}$ atoms/cm$^2$ fluorine. The damage profile is Gaussian in shape and representative of vacancy events that occur in the silicon substrate during the fluorine implant. As vacancies are created, dangling, strained, and weak silicon bonds are generated. The damage profile resulting from a 60 keV, $1\times10^{15}$ atoms/cm$^2$ germaium preamorphization implant is greater in concentration than the fluorine damage profile shown in Fig. 7 and extends beyond a depth of 1000 Å.[26] These results demonstrate that dangling and strained silicon bond distributions have Gaussian profiles. The shallower substrate regions have a greater propensity for defect trapping site passivation, thus allowing more mobile species. At greater depths, the damage cascades and the concentrations of incorporated species taper

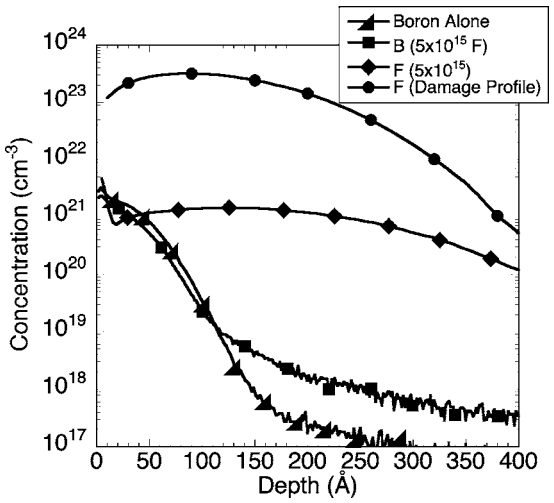


FIG. 7. Simulated damage profile for a 6 keV, $5\times10^{15}$ atoms/cm$^2$ fluorine implant, shown with dopant concentration profiles for as-implanted samples receiving 500 eV, $1\times10^{15}$ atoms/cm$^2$ boron with and without co-implanted 6 keV, $5\times10^{15}$ atoms/cm$^2$ fluorine.

off.[38] As a result, fewer trapping sites are removed and fewer atoms are mobilized.[33,34] Hobler *et al.*[33] and Hobler and Otto[34] studied and developed process simulators that successfully model the effects of implantation damage in silicon. They found that implantation collision cascades have the ability to stabilize existing defects through recombination, lowering the total defect population. The probability for defect recombination must be greater than that of survival in order for passivation to occur. Recent calculations suggest that the probabilities for recombination and survival are both system and species dependents.[34] Our samples were sequentially implanted with germanium, fluorine, and then boron. The population of dangling silicon bonds and defect trapping sites is expected to decrease with each dopant implantation step. During the initial implantation step, germanium ions amorphize the silicon substrate, creating a dangling silicon bond population on the order of approximately $1\times10^{19}$ sites/cm$^3$. The damage profile of the fluorine doping implant overlaps with the existing defect population and stabilizes many of the dangling silicon bonds generated during the amorphization process via recombination with fluorine and germanium atoms. Boron is the second dopant introduced into the system and is exposed to fewer trapping sites, as the majority of the defect population was eliminated by the preceding fluorine damage cascade. Boron atoms are expected to diffuse in regions where the dangling silicon bond population is low. Experimentally, our specimens demonstrate boron motion in the profile tail region, corresponding to depths where the fluorine and germanium damage profiles exhibit the greatest overlap. The theory of defect and trapping site passivation applies well to our experimental observations, adequately modeling the overall shift of the boron concentration profiles and footing of the tail region.[33,34,38]

Recent works suggest that germanium interaction with surrounding boron or fluorine atoms are unlikely within our samples. Ajmera *et al.*[39] characterized a germanium effect, whereby boron implants completely contained within the amorphous layer exhibit decreasing motion during annealing with increasing germanium preamorphization dose. This effect is believed to be chemical in nature, involving Ge–B pairing or clustering. By interacting with constituent boron, germanium retards boron motion rather than enhancing it. In addition, Hattendorf *et al.*[40] demonstrated that the binding forces between boron and germanium are not strong enough to promote Ge–B pair formation at temperatures below 600 °C in silicon-rich SiGe material. While reactions with fluorine are indeed possible, Ge–F clusters or pairs have not been shown to subsequently mobilize boron. These results support the assertion that germanium and fluorine promote boron motion in as-implanted material by passivating the dangling silicon bond population.

During the SPER process, germanium and fluorine dopant atoms maintain the same roles regarding boron diffusion. The fluorine atoms indirectly influence boron diffusion by controlling the total exposure time to amorphous material at elevated temperatures. We observed that boron has the ability to diffuse in germanium-preamorphized silicon at elevated temperatures during SPER without the assistance of any additional dopants, similar to that recently reported by Duffy *et al.*[4] The mere presence of germanium enables boron to diffuse during annealing at concentrations reaching $1\times10^{20}$ atoms/cm$^3$. At elevated temperatures, fluorine is known to intermingle with the mobile $a/c$ silicon interface.[31] These observations imply that chemical interactions between silicon and germanium are highly favorable during SPER, essentially reducing the formation energy of mobile boron. Diatomic bond enthalpy data suggest that silicon is equally as likely to interact with germanium atoms as with other silicon atoms.[41,42] Silicon is also less likely to interact with boron than with itself.[41,43] The systematic interaction of germanium and silicon enables boron to diffuse in amorphous silicon at elevated temperatures in both low and high concentration regions.

## SUMMARY AND CONCLUSIONS

The precise mechanisms by which enhanced boron diffusion occurs are rather complex and highly dependent upon several factors. The choice of silicon or germanium preamorphization species, the presence or absence of fluorine, and the incorporation or exclusion of activation annealing all affect boron diffusion in amorphous silicon.

In as-implanted material, fluorine-enhanced boron diffusion is observed for both germanium and silicon preamorphizations. Roughly five times more anomalous boron diffusion occurs in the former case. Chemical reactions between silicon and fluorine also contribute modestly to the observed motion, enabling boron atoms to become mobile at concentrations up to $1\times10^{19}$ atoms/cm$^3$ in germanium-amorphized substrates.

During the SPER process, boron can diffuse in germanium-amorphized material in the absence of additional dopants. Under these conditions, fluorine simply alters the regrowth rate of silicon, controlling the amount of time boron is exposed to amorphous material at elevated temperatures. The boron diffusivity during annealing is independent

of the fluorine dose. Mobile boron concentrations up to $1 \times 10^{20}$ atoms/cm$^3$ are observed during annealing at 550 °C.


[1] D. F. Downey, J. W. Chow, E. Ishida, and K. S. Jones, Appl. Phys. Lett. **73**, 1263 (1998).
[2] K. Ohyu, T. Itoga, and N. Natsuaki, Jpn. J. Appl. Phys. **29**(3), 457 (1990).
[3] L. S. Robertson, P. N. Warnes, K. S. Jones, S. K. Earles, M. E. Law, D. F. Downey, S. Falk, and J. Liu, Mater. Res. Soc. Symp. Proc. **610**, B4.2.1 (2001).
[4] R. Duffy *et al.*, Appl. Phys. Lett. **84**, 4283 (2004).
[5] J. M. Jacques *et al.*, Mater. Res. Soc. Symp. Proc. **810**, C10.3.1 (2004).
[6] D. Lecrosnier, J. Paugam, and J. Gallou, Appl. Phys. Lett. **30**, 323 (1977).
[7] R. G. Wilson, J. Appl. Phys. **54**, 6879 (1983).
[8] A. E. Michel, R. H. Kastl, S. R. Mader, B. J. Masters, and J. A. Gardner, Appl. Phys. Lett. **44**, 404 (1984).
[9] T. O. Sedgwick, A. E. Michel, V. R. Deline, S. A. Cohen, and J. B. Lasky, J. Appl. Phys. **63**, 1452 (1988).
[10] A. E. Michel, M. Numan, and W. K. Chu, Appl. Phys. Lett. **53**, 851 (1988).
[11] M. Kase, M. Kimura, H. Mori, and T. Ogawa, Appl. Phys. Lett. **56**, 1231 (1990).
[12] J. M. Jacques, L. S. Robertson, K. S. Jones, M. E. Law, M. Rendon, and J. Bennett, Appl. Phys. Lett. **82**, 3469 (2003).
[13] M. H. Clark, K. S. Jones, T. E. Haynes, C. J. Barbour, K. G. Minor, and E. Andideh, Appl. Phys. Lett. **80**, 4163 (2002).
[14] S. Roorda, J. S. Custer, W. C. Sinke, J. M. Poate, D. C. Jacobson, A. Polman, and F. Spaepen, Nucl. Instrum. Methods Phys. Res. B **59/60**, 344 (1991).
[15] T. Gebel, M. Voelskow, W. Skorupa, G. Mannino, V. Privitera, F. Priolo, E. Napolitani, and A. Carnera, Nucl. Instrum. Methods Phys. Res. B **186**, 287 (2002).
[16] H. Tsukamoto, Solid-State Electron. **43**, 487 (1999).
[17] G. Fortunato *et al.*, Nucl. Instrum. Methods Phys. Res. B **186**, 401 (2002).
[18] M. H. Juang, F. S. Wan, H. W. Liu, K. L. Cheng, and H. C. Cheng, J. Appl. Phys. **71**, 3628 (1992).
[19] S. Baek, T. Jang, and H. Hwang, Appl. Phys. Lett. **80**, 2272 (2002).
[20] M. H. Juang and H. C. Cheng, Appl. Phys. Lett. **60**, 2092 (1992).
[21] V. Privitera, C. Spinella, G. Fortunato, and L. Mariucci, Appl. Phys. Lett. **77**, 552 (2000).
[22] E. Napolitani, A. Coati, D. De Salvador, A. Carnera, S. Mirabella, S. Scalese, and F. Priolo, Appl. Phys. Lett. **79**, 4145 (2001).
[23] J. M. Jacques, L. S. Robertson, M. E. Law, K. S. Jones, M. J. Rendon, and J. Bennett, Mater. Res. Soc. Symp. Proc. **717**, C.4.6.1 (2002).
[24] E. Napolitani, A. Carnera, V. Privitera, and F. Priolo, Mater. Sci. Semicond. Process. **4**, 55 (2001).
[25] E. Napolitani, D. De Salvador, R. Storti, A. Carnera, S. Mirabella, and F. Priolo, Phys. Rev. Lett. **93**, 055901 (2004).
[26] J. F. Ziegler and J. P. Biersack, *The Stopping and Range of Ions in Matter (SRIM-2000.4)* (IBM Co., Maryland, 1999).
[27] I. Suni, G. Goltz, M. G. Grimaldi, M. A. Nicolet, and S. S. Lau, Appl. Phys. Lett. **40**, 269 (1982).
[28] I. Suni, G. Goltz, M. A. Nicolet, and S. S. Lau, Thin Solid Films **93**, 171 (1982).
[29] I. Suni, U. Shreter, M. A. Nicolet, and J. E. Baker, J. Appl. Phys. **56**, 273 (1984).
[30] J. Faure, A. Claverie, L. Laanab, and P. Bonhomme, Mater. Sci. Eng., B **22**, 128 (1994).
[31] I. Suni, U. Shreter, M. A. Nicolet, and J. E. Baker, J. Appl. Phys. **56**, 273 (1984).
[32] W. Frentrup and A. Mertens, Physica B **208/209**, 389 (1995).
[33] G. Hobler, A. Simionescu, L. Palmetshofer, C. Tian, and G. Stingeder, J. Appl. Phys. **77**, 3697 (1995).
[34] G. Hobler and G. Otto, Mater. Sci. Semicond. Process. **6**, 1 (2003).
[35] P. A. Thomas, M. H. Brodsky, D. Kaplan, and D. Lepine, Phys. Rev. B **18**, 3059 (1978).
[36] D. Kalpan, N. Sol, G. Velasco, and P. Thomas, Appl. Phys. Lett. **33**, 440 (1978).
[37] M. H. Brodsky and D. Kaplan, J. Non-Cryst. Solids **32**, 431 (1979).
[38] *Ion Implantation Science and Technology*, 2004 ed., edited by J. F. Ziegler (Ion Implantation Technology Co., New York, 2004), pp. 5-8–5-10.
[39] A. C. Ajmera, G. A. Rozgonyi, and R. B. Fair, Appl. Phys. Lett. **52**, 813 (1998).
[40] J. Hattendorf, W. D. Zeitz, W. Schroder, and N. V. Abrosimov, Physica B **340–342**, 858 (2003).
[41] C. Chatillon, M. Allibert, and A. Pattoret, C. R. Seances Acad. Sci., Ser. C **280**, 1505 (1975).
[42] A. G. Gaydon, *Dissociation Energies and Spectra of Diatomic Molecules*, 3rd ed. (Chapman & Hall, London, 1968).
[43] G. Verhaegen, F. E. Stafford, and J. Drowart, J. Chem. Phys. **40**, 1622 (1964).